

Diffraction Group(Annual Report)

journal or publication title	The science reports of the Tohoku University. Ser. 8, Physics and astronomy
volume	8
number	1
page range	65-72
year	1987-07-15
URL	http://hdl.handle.net/10097/25646

Diffraction Group

Academic Staff

Professor	Denjiro Watanabe
Associate Professor	Michiyoshi Tanaka
Research Physicists	Rokuro Miida and Osamu Terasaki

Technical Staff	Futami Sato
Secretary	Megumi Akasaka
Graduate Students	Masami Terauchi (D1) Toshikatsu Kaneyama, Hideki Suzuki and Tatsuhiko Tajima (M2) Shigeyuki Ito, Tomio Sato and Kenji Yamazaki (M1)
Research Student	Susumu Suzuki

Research Activities

(I) MAGNETIC DOMAIN STRUCTURES AT THE hcp/dhcp INTERFACE IN Co AND Co-Fe ALLOYS (D. Watanabe and H. Suzuki)

Ferromagnetic Co-Fe alloys with 0.8-1.2 at.% Fe generally contain stacking faults and consist of the two phases (hcp and dhcp), depending on heat-treatment and composition. Although saturation magnetization of the two phases is almost the same, there is a notable difference in the easy magnetization direction: it is parallel to the c-axis in hcp phase at room temperature and is in the c-plane in dhcp phase. Therefore, it is of interest to observe magnetic domain structures in the crystals consisting of the two-phases, and single crystals with the (11 $\bar{2}$ 0) orientation have been examined by the defocused mode of Lorentz microscopy, using the 1000 kV electron microscope. Two types of domain structure, i.e., wineglass-shape domains (walls) and spike domains, are frequently observed at the interface of the two phases.

In the wineglass-shape domain, domain wall along the c-axis in the hcp region broadens near the interface, forming wineglass-shape wall, and connects with bow-shaped wall in the dhcp region. Contrast of the stacking faults perpendicular to the c-axis bends near walls in the Lorentz image, owing to the effect of Lorentz deflection on the fault contrast, caused by magnetization component parallel to the [1 $\bar{1}$ 00]. Analysing the bending of fault contrast, magnetization distribution near the interface is obtained. As the wall in hcp region is approaching the interface, magnetization near

the wall deviates from the c-axis, maximum deviation angle θ being about 25° at the interface. Within the wall, it rotates by $\pi-2\theta$, satisfying the condition that the normal component is continuous across the wall. Existence of bow-shaped wall in the dhcp region is necessary to maintain the continuity of magnetization at the interface.

Spike domains are observed in the hcp region at the interface. Magnetization distribution near the domain, derived from the analysis of bending of fault contrast, is not so simple as that proposed for the spike domains observed on the axial plane at the bulk crystal edge parallel to the c-plane of hcp Co. Magnetization deviates from the c-axis within and near the domain, the maximum deviation angle being about 10° near the domain tip.

Single crystal of hcp Co with the $(11\bar{2}0)$ orientation was examined also, and domain structures similar to those mentioned above were observed at the crystal edge parallel to the c-plane.

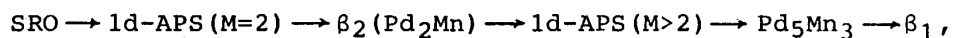
(II) SUPERSTRUCTURES IN THE Pd-Mn SYSTEM

(D. Watanabe, R. Miida and T. Tajima)

Ordered phases existing in the Pd-rich Pd-Mn system were studied by means of electron diffraction and X-ray powder diffraction methods, in order to clarify unresolved problems of the phase diagram, and the following results were obtained.

At temperatures above 700°C , the structure transforms from the short-range ordered state (SRO) to the one-dimensional antiphase domain structure (1d-APS, Pd_3Mn) based on Ll_2 lattice, when Mn-content increases from 25 to about 30 at.%. With further increase in Mn-content, the 1d-APS transforms continuously into the β_1 (PdMn) phase with Ll_0 lattice, without forming two-phase region, $\text{Pd}_3\text{Mn} + \beta_1$.

At temperatures below 700°C , however, the structure changes in the following sequence when Mn content increases from 25 to 40 at.%:



where, M denotes antiphase domain size in terms of lattice constant of the basic Ll_2 lattice.

(III) MARTENSITE TRANSFORMATION IN $\text{Au}(\text{Mn}_{1-x}\text{Zn}_x)$ ALLOYS

(O. Terasaki and D. Watanabe)

The β -phase AuMn transforms martensitically into tetragonal or orthorhombic at temperatures above room temperature. The specimen quenched by normal method gives a well defined banded structure of twin relation, and lattice distortion ϵ , $1 - c/a(c/b)$, changes in a stepwise from $+\epsilon$ to $-\epsilon$ at twin boundaries. On the other hand, the rapidly quenched (RQ) specimen does not give well defined twin boundaries in this region. ϵ , measured from an

HREM image, changes gradually from $+\epsilon$ to $-\epsilon$ within the region of several tens Å which is similar to the twin boundaries in ferroelastic materials (ϵ changes in a form of $\sim \tanh sx$). Peculiar line contrast running parallel to $\{100\}$ is also observed in the EM images obtained from RQ specimen. The lines are aligned periodically and the distance between them is ca 20-30 nm. It is concluded from the analysis of the image that the specimen bends periodically in a form of $\sim \cos hx \cdot \cos ky$, and the conditions to produce the bending in such a way through the stress induced by martensite transformation are under consideration.

It has been reported that martensite transformation temperature decreases with the replacement of Mn by Zn, down to room temperature at Au ($\text{Mn}_{0.52}\text{Zn}_{0.48}$). To observe pre-transformation and dynamic phenomena by electron microscopy, specimens of $\text{AuMn}_{1-x}\text{Zn}_x$ with $x = 0.4-0.52$ were prepared by normal and RQ methods. We observed extra spots in electron diffraction patterns from Au(Mn,Zn) alloys instead of β -phase pattern.

(IV) TRIAL TO INSERT ATOMIC STRINGS OF Se INTO THE CHANNELS OF ZEOLITES (O. Terasaki, K. Yamazaki and D. Watanabe)

It has been realized that relatively few of the investigated low-dimensional solids exhibit genuine one- or two-dimensional behaviour. One possible way to make one-dimensional material is to accommodate individual atomic chains within the well ordered pores of atomic size. The aims of the present work are to insert atomic strings into the channels of zeolites, to characterize them and finally to lead to observe the properties which are characteristic in low dimension. We tried to insert the chains of Se thermally into synthetic mordenite, a zeolite which has one-dimensional channels (dia. ca 7 Å) running parallel to its c-axis, after Bogomolov et al. The white mordenite was converged into an orange colour. We successfully observed the chains of Se setting in the main channels by HREM images, and also observed patchwise contrast corresponding to the density modulation of Se along the b-axis with a periodicity of about 100 Å. The trials to insert Se into other zeolites to find the effects of the size and dimensionality of channels, which give the restricted geometry condition, are under progress.

(V) CONDITIONS FOR OBSERVING INVERSION CENTRES IN ZSM-5 AND METAL IONS IN ZEOLITE Y (O. Terasaki and D. Watanabe)

The aim of this study is to find conditions to enhance and pick up the structure informations we need in HREM images.

It is quite important subject to study the possibility of periodic intergrowth of ZSM-5 and ZSM-11. They are closely related to each other in structure, and the symmetries of projected structure along the straight channels, $[010]$, are pgg and cm , respectively. HREM images have been observed

to show not mirror but twofold symmetry at overfocus in thin part of specimen and at underfocus in thick region by enhancing the relation $F(h0\ell) = -F(h0\bar{\ell})$ where $h+\ell = 2n+1$.

Dependence of the HREM images on the diffracted beams that go through the objective aperture is employed to observe the effect of Ag cations on the EM images. Although we can easily see the effect of Ag in projected potential density, we found that best resolution which is obtainable at present stage does not give the information about Ag cation but lower resolution may be preferable by tuning the objective aperture size just to include the reflections which mainly come from Ag cations.

(VI) CONVERGENT-BEAM ELECTRON DIFFRACTION (CBED)

a. Dynamic Extinction (M. Tanaka, M. Terauchi and H. Sekii)

The rules for dynamic extinction in electron diffraction, occurring in kinematically forbidden reflections due to screw axes or glide plane, were given by Gjønnes and Moodie (Acta Cryst. 19 (1965) 65). Among the rules, the dynamic extinction due to a glide plane which is set perpendicular to the incident beam was predicted to appear as a dark spot at the exact Bragg position of a kinematically forbidden reflection due to the plane. This extinction was observed for the first time in the 420 reflection of spinel and the 200 reflection of silicon using convergent-beam electron diffraction. On the basis of experimental results, the rule for the glide plane given by Gjønnes and Moodie was modified as follows: the extinction occurs as dark lines crossing at the exact excitation position.

b. Determination of Burgers Vector

(M. Tanaka, T. Kaneyama and A. Ishikawa)

The principle of determining Burgers vector **b** of a dislocation was given by Cherns and Preston (Proc. XIth Int. Cong. on Electron Microscopy, Kyoto, 1986, p.203). We carried out two-beam dynamical calculations of the intensity profiles of high-order reflections **g** which are across a dislocation line and have various integral values of **g·b**. A reflection line has n-nodes at the crossing region with the dislocation when the value of **g·b** equals to n. The sign of the product **g·b** plays an important role for the determination of Burgers vector. The shape of nodes for +n has an opposite sense to that for -n. The values and the sign of **g·b** = n for three non linear reflections which are across the dislocation line enable to determine Burgers vector of the dislocation. Examples of the determination were demonstrated for dislocations in aluminum. Further, we revealed that partial dislocations and dislocation dipoles can be determined by the extensive application of the Cherns method.

c. $\text{Al}_{74}\text{Mn}_{20}\text{Si}_6$ (M. Tanaka and M. Terauchi)

Convergent-beam electron diffraction and small-area-parallel-beam electron diffraction have revealed the crystallographic nature of icosahedral quasicrystals in a melt-quenched $\text{Al}_{74}\text{Mn}_{20}\text{Si}_6$ alloy. This quasicrystal possesses a much greater ordering in its atomic arrangement than an Al_6Mn quasicrystal. The present alloy was found to have a very high Debye-temperature. The point group was determined to be centrosymmetric $m\bar{3}5$, although a small breakdown of mirror symmetry was observed. Small-area-parallel beam electron diffraction patterns taken with the incidence along the fivefold axis showed a characteristic deviation from the tenfold symmetry. It was shown that the patterns with the deviation could be explained by usual crystallography without the introduction of the quasicrystalline order.

d. SrTiO_3 (M. Tanaka and M. Terauchi)

Last year we found that the space group of the low temperature phase of SrTiO_3 is $I4cm$ for the crystals grown by the Verneuil method. It was suggested that the growth by the method can destroy the intrinsic and delicate symmetry of the phase. We reexamined the space group of the crystals grown by the flux method and found the space group to be $I4/mcm$, which must be the intrinsic symmetry and is the same with that determined by neutron diffraction.

e. $\text{BaPb}_x\text{Bi}_{1-x}\text{O}_3$ (M. Tanaka and K. Tsuda)

The space group of an oxide superconductor $\text{BaPb}_x\text{Bi}_{1-x}\text{O}_3$ was studied. Possible space groups were $Pmmm$ and $Pmm2$. Breakdown of an inversion center is very small even if it exists.

(VII) SUPER-IONIC CONDUCTOR (R. Miida, S. Suzuki and M. Tanaka)

Lattice Modulation in the $\text{Bi}_2\text{O}_3\text{-Nb}_2\text{O}_5$

It had been reported that the fast-ion-conductor $(\text{Bi}_2\text{O}_3)_{1-x}(\text{Nb}_2\text{O}_5)_x$ ($0.13 \leq x \leq 0.24$) had the fluorite (CaF_2) - type structure, in which the cation- and anion-sublattices were occupied at random with $\text{Bi}_{1-x}\text{Nb}_x$ and $\text{O}_{0.75+0.5x}$ $\square_{0.25-0.5x}$ (\square = vacancy), respectively. We found a modulated structure in the system and constructed a structural model using electron diffraction, high-resolution electron microscopy and X-ray powder diffraction. Electron diffraction patterns showed many extra spots as well as fundamental spots expected from the CaF_2 -type structure. The extra spots characteristic of the modulated structure are located at $nq\mathbf{k}_{111}$ ($n=1,2,\dots$) and the equivalent positions allowed by a cubic symmetry, where \mathbf{k}_{111} is the 111-reciprocal lattice vector. We found that the value of q increases continuously from 0.360 to 0.383 with increasing x from 0.13 to 0.24. Together with these spots,

weak spots were observed at $m\mathbf{k}_{111} + n\mathbf{k}_{\bar{1}\bar{1}\bar{1}}$ ($m, n = 1, 2, \dots$) and the equivalent positions. The spots at \mathbf{qk}_{200} ($= \mathbf{qk}_{111} + \mathbf{qk}_{\bar{1}\bar{1}\bar{1}}$), \mathbf{qk}_{020} and \mathbf{qk}_{002} were found to occur from double diffraction. Relative intensities of all the extra spots increased with x . Crystal structure images taken from the specimens with $x = 0.15$ and 0.20 made clear that no incommensurate wave but a mixture of two commensurate waves with the period of $2d_{111}$ and $3d_{111}$ ($d_{111} = 1/|\mathbf{k}_{111}|$) exists. The mean period of the mixture measured from the structure images showed a fairly good agreement with $1/|\mathbf{qk}_{111}|$ observed in the diffraction patterns. X-ray intensity measurements of hhh reflections ($h = q, 1-q, 1$ and 2) were made for $(\text{Bi}_2\text{O}_3)_{0.79}(\text{Nb}_2\text{O}_5)_{0.21}$ with $q = 0.375$. It was revealed from the relative intensities of these reflections that modulated concentration waves exist on both the cation- and anion-sublattices. A structural model was constructed so as to reproduce the relative X-ray intensities of those reflections and the extinctions of reflections observed in electron diffraction patterns.

(VIII) HIGH RESOLUTION ENERGY-ANALYSIS

(M. Tanaka, M. Terauchi and F. Sato)

The Wien filter has electric and magnetic fields which are crossed perpendicularly. When the magnetic field has a linear gradient and the electric field is homogeneous, the filter achieves a stigmatic focus for incident electrons under the Wien condition of $E/B = v$ without consideration of the fringing fields, where E , B and v are the electric field strength, the magnetic field strength, and the velocity of the incident electrons. A Wien filter, the shapes of the magnetic pole pieces and electrodes, was designed so as to realize the stigmatic focus. However, it was found that the fringing fields destroy the Wien condition and the stigmatic focus. The geometry of the filter was modified so as to hold almost the Wien condition even in the fringing fields, then electrons again running straight on and having the stigmatic focus.

Publications

- 1) Observation of Magnetic Domains in Cobalt and Fe_3Al by Lorentz Microscopy, D. Watanabe, In Situ Experiments with High Voltage Electron Microscopes, Osaka University, 1986, pp. 421.
- 2) Magnetic Domains in Ferromagnetic Alloys with Structural Inhomogeneity Studied by High Voltage Lorentz Electron Microscopy, D. Watanabe, H. Suzuki and T. Sato, Proc. XIth Int. Cong. on Electron Microscopy, Kyoto, 1986, p. 977.
- 3) Accurate Measurement of Crystal Structure Factor by Electron Diffraction, D. Watanabe, *Ōyo-Butsuri* 55 (1986), 953 (in Japanese).

- 4) Electron Microscopic Study on the Structure of Au-Mn Alloys ($\text{Au}_2\text{Mn} - \text{Au}_3\text{Mn}_2$), T. Aiba, O. Terasaki and D. Watanabe, Proc. XIth Int. Cong. on Electron Microscopy, Kyoto, 1986, p. 873.
- 5) Conditions for Observing Inversion Centres in ZSM-5 and Metal Ions in Zeolite Y, O. Terasaki, M.K. Uppal, G.R. Millward, J.M. Thomas and D. Watanabe, Proc. XIth Int. Cong. on Electron Microscopy, Kyoto, 1986, p. 1777.
- 6) Anomalous Contrast in Electron Microscope Image Obtained from Rapidly Quenched Au-Mn Alloy, O. Terasaki and D. Watanabe, Proc. Int. Conf. on Martensite Transformations, Nara, 1986, p. 1115.
- 7) Electron Microscopic Study on the Fine Structures of Zeolites, O. Terasaki and D. Watanabe, Shokubai (Catalyst) 28 (1986), 550 (in Japanese).
- 8) CBED Studies of Imperfect Crystals, M. Tanaka and T. Kaneyama, Proc. XIth Int. Cong. on Electron Microscopy, Kyoto, 1986, p. 203.
- 9) Convergent- and Small-Area-Parallel-Beam Electron Diffraction of Icosahedral Quasicrystals, M. Tanaka, M. Terauchi, K. Hiraga and M. Hirabayashi, Proc. XIth Int. Cong. on Electron Microscopy, Kyoto, 1986, p. 171.
- 10) Space Group Determination of Psuedo One Dimensional Compound TaS_3 , M. Tanaka and T. Kaneyama, Proc. XIth Int. Cong. on Electron Microscopy, Kyoto, 1986, p. 723.
- 11) Simultaneous Observation of Zone-Axis Pattern and $\pm\text{G}$ Dark-Field Patterns in CBED, M. Terauchi and M. Tanaka, Proc. XIth Int. Cong. on Electron Microscopy, Kyoto, 1986, p. 693.
- 12) Electron Optical Studies of the Mobile-Ion Arrangement in Hollandites, S. Suzuki, M. Tanaka, M. Ishigame, T. Suemoto, Y. Shibata, Y. Onoda and Y. Fujiki, Proc. XIth Int. Cong. on Electron Microscopy, Kyoto, 1986, p. 1717.
- 13) Conventional Transmission-Electron Microscopy Techniques in Convergent-Beam Electron Diffraction (Review), M. Tanaka, J. Electron Microsc. 35 (1986), 314.
- 14) A New Technique in Convergent-Beam Electron Diffraction, M. Tanaka and M. Terauchi, Nihon-Denshi News 26 (1986), 58 (in Japanese).
- 15) Simultaneous Observation of a Zone-Axis Pattern and $\pm\text{G}$ Dark-Field Patterns in Convergent-Beam Electron Diffraction, M. Tanaka and M. Terauchi, JEOL News 24E (1986), 62.
- 16) Diffraction Study of Al-Mn and Al-Mn-Si Quasicrystalline Alloys, M. Tanaka and M. Terauchi, Solid State Physics 22 (1987), 193 (in Japanese).
- 17) *Dictionary of Surface Analysis*, M. Tanaka, ed. M. Okada, Kyoritsu-Shuppan, 1986, pp. 386 (in Japanese).

- 18) Observation of Dynamic Extinction due to a Glide-Plane Perpendicular to the Incident-Beam by Convergent-Beam Electron Diffraction, M. Tanaka, M. Terauchi and H. Sekii, *Ultramicroscopy* 21 (1987), 245.
- 19) Electron Microscope and Diffraction Study on the γ -phase of Al-Ti Alloy System, R. Miida and D. Watanabe, *Proc. XIth Int. Cong. on Electron Microscopy*, Kyoto, 1986, p. 955.
- 20) One-Dimensional Antiphase Domain Structures in the Aluminum-Rich Al-Ti Alloys, R. Miida, *Jpn. J. Appl. Phys.* 25 (1986), 1815.

Master Theses (March 1987)

- 1) Identification of Stacking Faults and Dislocations by Convergent-Beam Electron Diffraction, Toshikatsu Kaneyama.
- 2) Magnetic Domain Structures at the hcp-dhcp Interface in Co-Fe Alloys, Hideki Suzuki.
- 3) Electron Diffraction and Electron Microscope Study on the Superstructures of Pd-Mn Alloys, Tatsuhiko Tajima.